

# A bi-directional electric vehicle charging system for experiential and public education

ANDREW WONG, BRIAN CHONOS, CESAR GARCIA,  
DENNIS NGUYEN, FERNANDO BARRERA, HA THU LE  
Department of Electrical and Computer Engineering,  
Cal State Polytechnic University, Pomona,  
Pomona City, California 91768,  
UNITED STATES OF AMERICA

*Abstract:* – As countries around the world transition to electric vehicles (EV), there is an urgent need to develop a workforce for this area where experiential training is indispensable. Further, public education of electric vehicles is also needed to accelerate adoption of the emission-free vehicles. To serve this purpose, a bi-directional charger for EVs has been designed, implemented in MATLAB Simulink, and built as a physical system. It visualizes EV charging action using computer-based simulation, as well as physical demo of the prototype. The testing results show that a bi-directional charger is not only possible to make but also can be readily used in the near future. The Simulink model shows that Grid-to-Vehicle and Vehicle-to-Grid operation modes work as desired to charge and discharge EV battery appropriately. The physical model confirms this finding. The study contributes a novel approach to EV-related training activities where both the software and physical models are developed for explaining advanced technical concepts, such as battery charging and discharging, microcontroller coding, voltage sensing, state of charge estimation, and converter operation. The Simulink model vividly visualizes the system operation using colorful graphics, which enhance learner understanding and interest in the subject. The physical model connects the theory with hands-on experience, which is a desired approach in current engineering education. The MATLAB Simulink charging and discharging models have been used to teach a graduate course in electric vehicle and energy storage successfully. Overall, both the simulation and the physical systems can be effective tools for EV-related experiential training and for educating the general public. This helps promote the usage of EV for the benefits of the power grid and EV owners, as well as reduce carbon emissions to protect the environment.

*Key-Words:* – Bi-directional charger, experiential training, public education, electric vehicle, grid to vehicle, workforce development, vehicle to grid.

Received: February 13, 2024. Revised: May 1, 2024. Accepted: May 15, 2024. Published: May 22, 2024.

## 1. Introduction

Transition from gasoline-powered cars to electric vehicles (EV) has been motivated by a series of incentives and regulations as part of vigorous efforts to reduce carbon emissions, [1-15]. In California, where the state law mandates that all newly produced vehicles are to be emission free starting 2035, electric automobiles from companies such as Tesla, Nissan, and Rivian have begun to grow in popularity as people have started moving away from normal combustion cars towards electric. However, a serious concern regarding this increasing usage of EVs is possible stress on power systems caused by EV high power demand. With more of these cars having to be charged on a daily basis, overall power consumption

will increase drastically, leading to a large burden on the power supply side, [9]. Uncoordinated charging routines are a main concern regarding pushing to zero-emission vehicles (i.e., electric vehicles) as they are detrimental to the power grid, [14]. Additionally, a greater number of electric automobiles causes more charging stations to be built, which creates difficulty for the electric power utilities to estimate how much energy to distribute to all parts of a city, [11], [15]. Lastly, battery charge depletes overtime unlike fuel in fuel tanks, so leaving electric vehicles stationary for long periods of time will result in energy being wasted and lost, [11], [12]. One way to alleviate these problems is incorporating a smart inverter system into each EV charger. This is to create a bi-directional

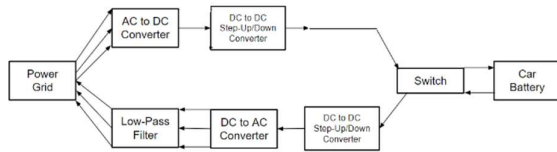


Fig 1 Diagram of EV bidirectional charging model

charging system that enables smart charging and discharging where the EV battery power can be channeled back to the grid to support it at times of needs.

Bidirectional chargers are a relatively new type of technology that have been increasingly researched into. They can operate in two ways: (i) drawing AC power from the grid and converting it to DC for charging the car battery (known as G2V, or grid-to-vehicle) or (ii) taking DC power from the battery and sending it back as AC (known as V2G, or vehicle-to-grid). G2V is already common with all charging stations where the speed in which they charge varies. The varying charging speed and time can be broken into three levels based on the input voltage required, [7]. Level 1 requires an input of 120V averaging around five miles per hour of charging. Level 2 requires 208V-240V and can provide 20-60 miles per hour. Level 3 DC fast charging takes place at 200-600VDC and provides 180-300 miles per hour. V2G can help stabilize the grid during sudden load peaks, as well as put sitting battery units to use, [4]. It can also create multiple benefits for EV owners. The ability of V2G incentivizes the EV owners by selling back power into the grid during peak times to earn extra income while buying power at a lower price when they charge their EV at night, [15]. While the two operations perform opposite tasks, incorporating a suitable control scheme would allow seamless transition between the two. Bi-directional charging will facilitate the grid to support the ever-growing EV industry.

Adoption of EVs and bi-directional charging would be accelerated by increasing experiential teaching of these subjects at colleges and universities, as well as general public education. Past experience obtained by Dr. Ha Thu Le, the advisor of this project, has shown that students and the general public have strong preference for hands-on learning and visual demonstration of new systems such as EV bi-directional chargers.

Based on the above analysis, this study aims to develop a simple-to-understand bidirectional charging system for experiential and public education. The system is first designed in a realistic manner and implemented in software to support computer-based learning. The realistic design is then scaled down and

built as a physical system that supports hands-on learning and public demonstration. The diagram of the bi-directional model is shown in Fig. 1.

## 2. Theoretical Design and Simulation

### 2.1 Theoretical Design

The theoretical design follows the model in Fig. 1 where major blocks are as follows.

- 1) *Power grid*: For residential applications, which is what this study is designing for, is a three-phase 60-Hz source that supplies two voltages, namely, 120V RMS line-neutral and 240V RMS line-line, [16].
- 2) *Low pass filter*: This can pass signals with a frequency lower than a selected cutoff frequency. It can be used to reduce noise and unwanted high frequency signals when converting AC to DC voltage or vice versa, [17]. The filter is of LC type.
- 3) *Rectifier/Inverter*: Rectifier converts AC to DC voltage for charging EV battery while inverter converts DC voltage to AC in discharging mode for channeling power back to the grid or supplying AC loads, [18].
- 4) *DC-DC converter*: This device converts one DC voltage to another DC voltage. The step-up converter is called a booster and the step-down is called a buck converter, [19]. Component values are calculated from the input voltage and the desired output voltage.
- 5) *EV battery*: Lithium-ion batteries are commonly used to power EV electric motors. In this study, the simulation model is based a Tesla Model S battery [20]. It has well-rounded specifications compared to other EVs such as Arciomoto and Rivian, [21]. The battery characteristics are obtained from [22] and [23].

### 2.2 MATLAB Implementation of Theoretical Design and Simulation Outcomes

#### *MATLAB Simulink implementation*

The battery used for simulation model is Tesla Model S battery, whose parameters are as follows.

Capacity (kWh)	100
Number of Cells	7,104
Modules Wired in series	16
Groups wired in series	6
Cells wired in series	96
Nominal Voltage (V)	400
Nominal Current (A)	250

The theoretical design is implemented using MATLAB Simulink by modifying a model in [22]. It results in a bi-directional charger where charging and discharging systems are separated. The systems are shown in Fig. 2.

**Charging system (Fig. 2, top):** It consists of an IGBT-based AC-DC converter and a boost converter which interface the 400-V battery with an AC 240-V source representing Level 2 charging. The AC-DC converter rectifies the AC voltage to DC while the booster raises the converter output voltage to a level suitable for the battery charging.

**Discharging system (Fig. 2, bottom):** It comprises of an IGBT-based AC-DC converter like that of the charging system and a boost converter which connect the 400-V battery to a 3-phase AC load rated 240V and 800W. The AC-DC converter is operated as a 3-phase inverter using a pulse width modulation technique. The carrier and reference signals are shown at the top of the diagram. The booster is used to increase the voltage input to the inverter. The battery is set to be fully charged for the simulation.

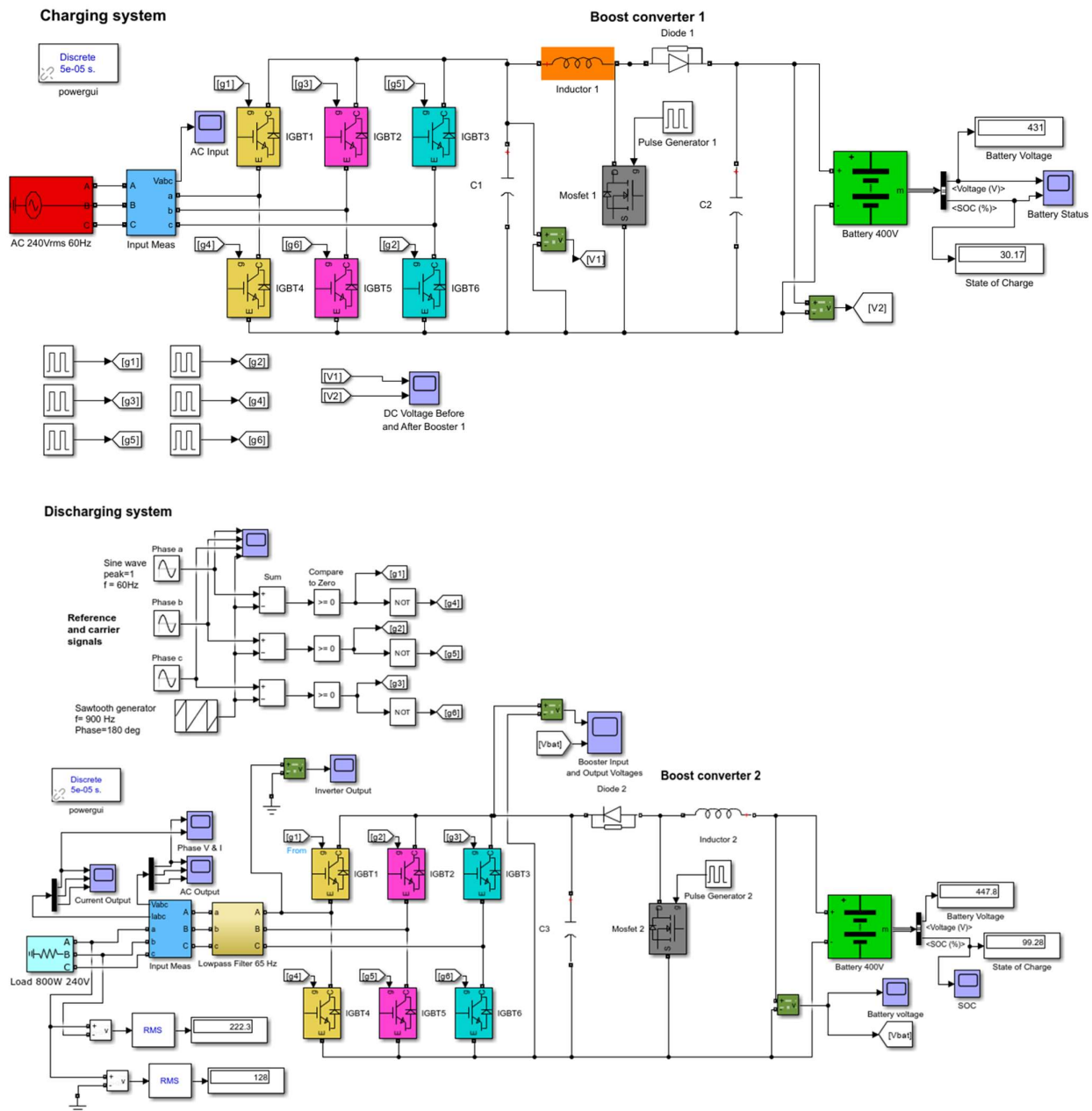


Fig. 2 Charging (top) and discharging (bottom) systems in MATLAB Simulink, [22].

The charging and discharging systems can be used separately to educate Grid-to-Vehicle and Vehicle-to-Grid operational modes of EV. The IGBT-based converter can be operated as a rectifier (charging operation) or as an inverter (discharging operation). They can also be combined to make a bi-directional charging system.

*Simulation outcomes*

The simulation outcomes showing how charging and discharging systems work are presented in Fig. 3, Fig. 4, Fig. 5, Fig. 6, Fig. 7 and Fig. 8.

*Charging system operation*

Figure 3 shows the voltage at the battery input terminals. The bottom figure shows the battery state of charge for simulation duration of 10s. It is visible that the battery is charging as the state of charge increases. The battery voltage is relatively stable.

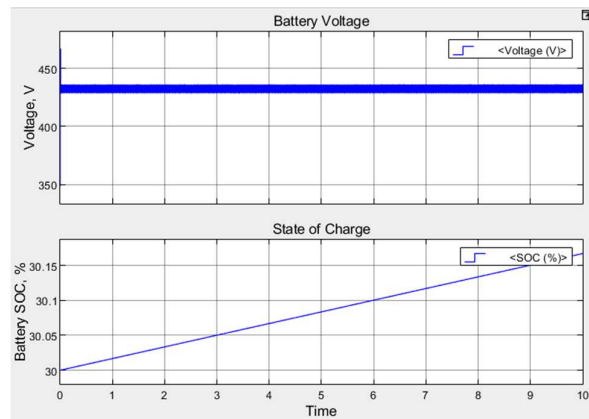


Fig. 3 Charging system – Battery voltage and state of charge.

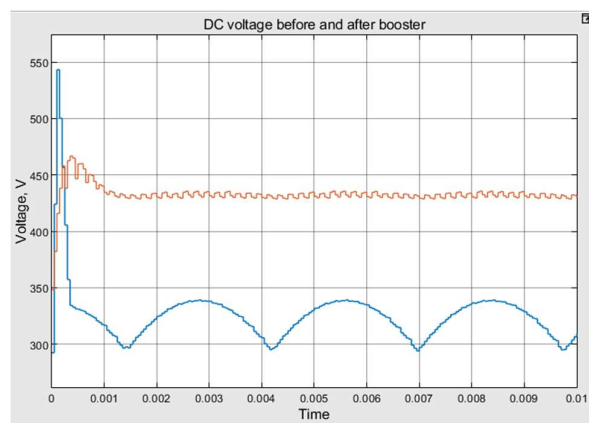


Fig. 4 Charging system – Booster operation plots showing DC voltage input to booster (bottom) and DC voltage output from booster (top).

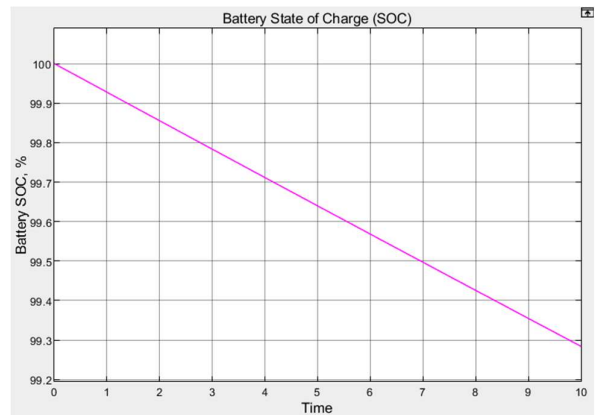


Fig. 5 Discharging system – Battery state of charge.

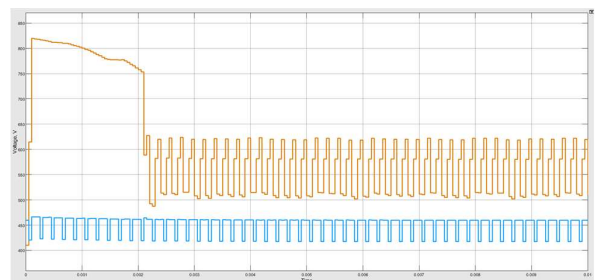


Fig. 6 Discharging system – Booster operation plots showing DC input voltage to booster (bottom) and DC voltage output from booster (top).

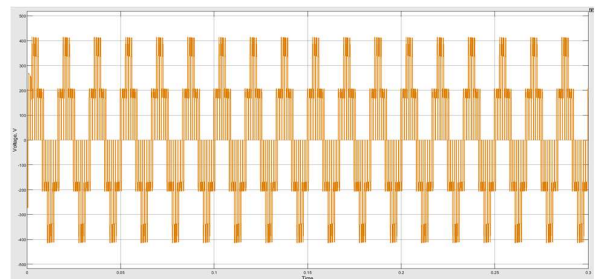


Fig. 7 Discharging system – Line-neutral AC voltage output from 3-phase inverter (DC-AC 6-bridge converter) which has lots of harmonics.

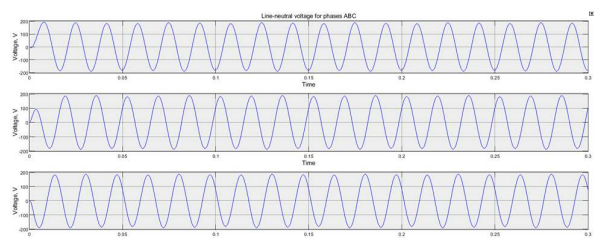


Fig. 8 Discharging system – 3-phase line-neutral AC voltage output from low-pass filter (voltage output to the 240-V 3-phase AC load); It is 60-Hz sinusoidal with very little harmonics.

Figure 4 shows the impact of the booster operation. The DC voltage input to the booster is the bottom plot and the DC voltage output from the booster is the top plot. It can be seen that the DC voltage input to the booster is lower than 350V and has considerable ripples. The booster increases the voltage to around 431V and reduces the ripples at the same time. As the result, the booster output voltage is appropriate for charging the battery whose voltage rating is 400V.

#### *Discharging system operation*

Figure 5 shows the state of charge of the battery when discharging. It is visible that the battery is outputting power to the load as the state of charge is decreasing.

Figure 6 illustrates the booster operation. The DC input voltage to the booster is the plot at the bottom and the DC voltage output from the booster is the top plot. Visibly, the booster increases the voltage input to the inverter. The goal of doing so is to increase the inverter output voltage to match the load voltage rating of 240V.

Figure 7 shows the waveform of the line-neutral AC voltage output from the 3-phase inverter. It has lots of harmonics which requires a filter to remove the harmonics.

Figure 8 shows the inverter line-neutral output voltage for Phases A, B and C, after being passed through the low-pass filter (Fig. 2, bottom). Most harmonics have been removed and the waveform become almost purely sinusoidal of 60Hz.

### **2.3 Application of Simulink models for experiential training**

The aforementioned Simulink charging and discharging systems have been used for teaching a graduate course named ECE 5990 “*Electric Vehicle and Energy Storage*” in Spring 2023. The course is developed and taught by Dr. Ha Thu Le, an author of this study. The course was sensational for both ECE graduate and undergraduate students. As the result, 42 students enrolled in the course, although the limit for a graduate course is 20.

During the course, the models were used to demonstrate the EV-related concepts, including battery charging and discharging, state of charge measurement, AC-DC and DC-DC converter operation, pulse width modulation, quantification of harmonics, and filter operation. At the end of the course, students were asked to design a relevant system, such as a charging or discharging system for electric vehicles, as a hands-on project.

Feedback received from student evaluation of the course shows that students were very interested in the subject. The course evaluation score was very good.

## **3. Physical System Design and Implementation**

For supporting hands-on learning and public demonstration, a scaled down version of the theoretical design is implemented using hardware (i.e., as a physical system).

### **3.1 Physical System Design**

The system components and its circuit diagram are shown in Fig. 9. The bi-directional charger follows the model in Fig. 1 where charging and discharging systems are separated and connected in parallel. A switch is used to toggle from charging mode to discharging mode. This design is advantageous for any educator/trainer who wants to demonstrate charging and discharging modes separately.

*Components of scaled-down model (Figures 9, 10, 11, 12):* The grid source for powering the charger is a regular 120-VAC American outlet. The battery is a li-ion 12.8-V, 256-W with a continuous discharge current of 20A and continuous charge current of 12A. The inverter is a pure sine power inverter that has a 12 VDC input, a 120-VAC output, and 180W/360W power output. The charge controller has an in-built rectifying circuit and voltage regulating circuit. This allows the charger to control the voltage and current input as well as output, allowing the charger to deliver the required voltage needed to charge the battery.

The battery is charged with the use of the constant current and constant voltage method, meaning that the charger first applies a constant current and then a constant voltage once the battery is almost at full capacity. The scaled-down physical model is not used to discharge the power from the battery back into the grid. Instead, it discharges into an electrical fan acting as an AC load, as shown in Fig. 10 and Fig. 11. The inverter comes with built in capacitance allowing for the fan to receive the appropriate real and reactive power to turn on.

To connect the charger and discharger into one system, a 12-V relay board is used to allow for a smooth switching from charging to discharging mode. The board has 2 relays, one for controlling charging (Relay 1) and the other for controlling discharging (Relay 2). An Arduino microcontroller reads the battery’s state of charge (SOC) to determine whether the system should be operated in charging or discharging mode.

Theoretically, the charger would be connected to the electrical grid and be charging the battery inside the electric vehicle. When the battery is at an appropriate charge level, under the owner’s command, the charger would switch to discharge

mode, sending power back into the grid. For the physical system, as mentioned before, sending power back into the grid was not possible so the AC electric fan is used as a substitute for the grid. Powering the fan demonstrates that the system could switch to discharge mode and use the battery to power up the fan. The physical system full list of components is provided in Table A1 of Appendix.

### 3.2 Microcontroller Logic, Code, and System Operation

The control logic flowchart (Fig. 13) depicts the logic of the code used in the microcontroller Arduino Uno R3 for operating the physical model.

The code enables the microcontroller to control when the system is charging or discharging, read the battery voltage for State of Charge calculations, and output information onto the LCD screen and LEDs. The controller constantly checks the battery terminal voltage, converts that to a SOC value, and outputs that value on the LCD screen (Fig. 12). The battery discharged curves used for determining its SOC are shown in Fig. 14.

Referring to Fig. 13, if the sensed SOC value is below a certain threshold (e.g. below 60%), the system will turn the first relay on and the second relay off to begin charging. If the SOC value is above a certain threshold (e.g. greater than 60%), the system will turn the first relay off and the second relay on to begin discharging. The thresholds can be changed by modifying the code. For preserving the battery life, discharging is not allowed if its SOC is 30% or lower. The battery SOC is constantly displayed by the LCD screen. The system operation mode is indicated by three LEDs where Green is charging, Red is discharging, and Blue is idle (not charging nor discharging).

A voltage divider is used to divide the battery voltage into a voltage tolerable by the microcontroller. Using the ADC read function, the voltage can be read from 0-5V in values from 0-1024. Using the battery discharge curve (Fig. 14), this can then be mapped based on the discharge curve. For instance, if the maximum voltage of the battery is 13.8V, and the ADC value read from that voltage is 900, then 900 is mapped to correspond with a 100% SOC. This process of mapping continues for all possible voltages from the battery.

One key point to note is that this mapping was done when the battery is not under load. While under load or charging, measurements are less accurate with  $\pm 5\%$  error. Another factor that impacts the

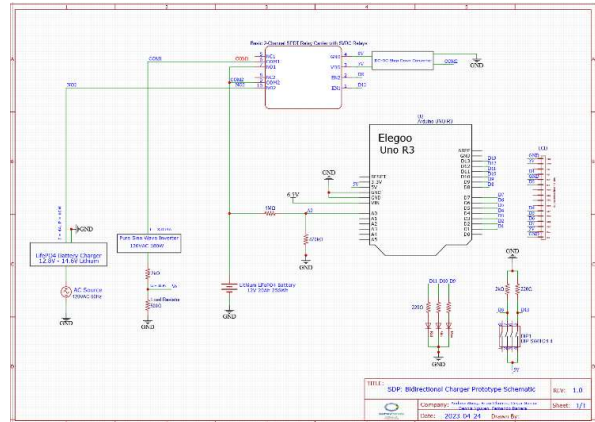


Fig. 9 Circuit diagram of physical bi-directional charger.

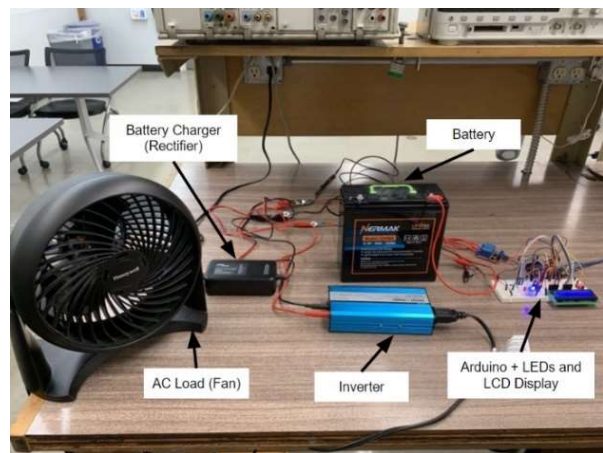


Fig. 10 Lab-based testing of physical bi-directional charger.

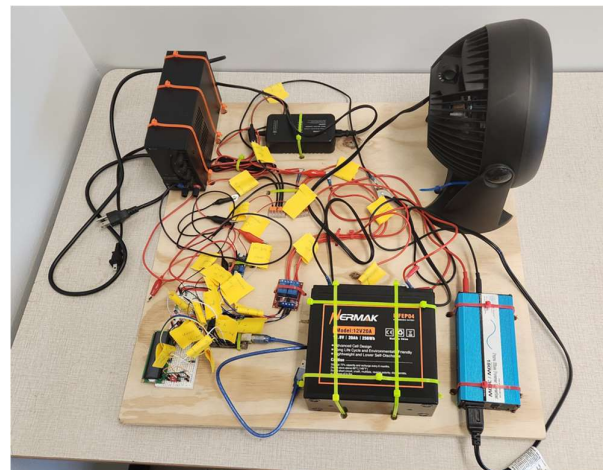


Fig. 11 Bi-directional charger mounted on a wooden base with annotated electrical connections for easy moving and training.

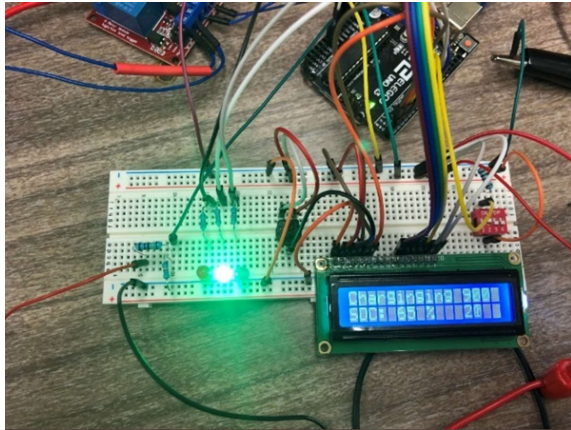


Fig. 12 Breadboard with LCD connected to microcontroller; the LCD displays the battery state of charge and operation mode.

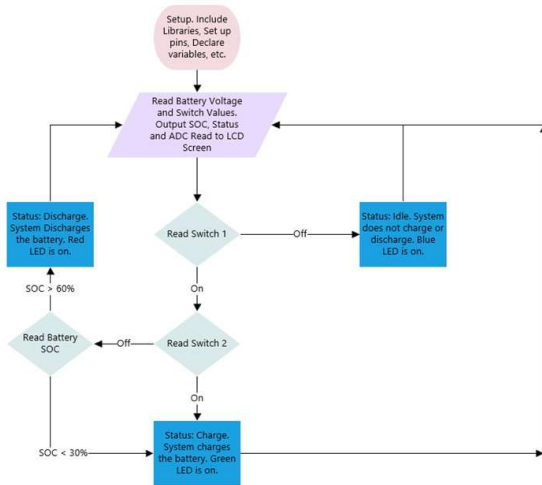


Fig. 13 Flowchart of microcontroller control logic.

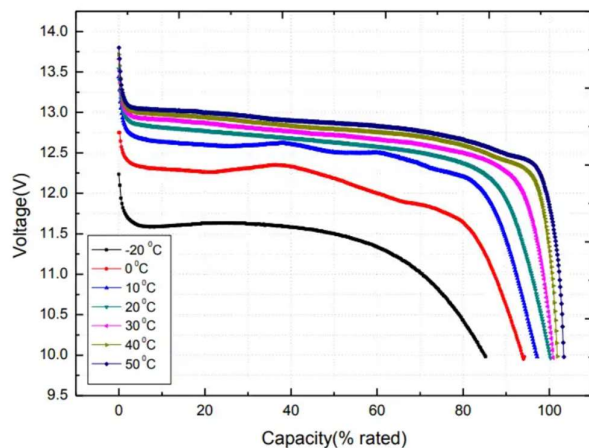


Fig. 14 LiFePO4 battery discharge curve [23].

accuracy is due to the fact that the discharge curves are not linear. Therefore, it is difficult to obtain highly accurate SOC estimates. Though, certain

inaccuracy of the SOC estimates would not significantly impact the system operation. For example, it is not a big error if the discharging mode is activated to output power to the grid at 60-percent SOC while the actual SOC is 59%. The complete microcontroller code is provided in Appendix.

#### 4. Testing of Physical System and Performance

Several tests were conducted for the physical system to learn if it functions properly.

*Test setting:* A 120-VAC outlet is used to charge the battery using the charger. Then, the battery is switched to discharging mode to supply either the AC fan or a resistive load. The system operation is observed by various indicators which are displayed by the LCD screen and LED. They include the battery SOC, operation mode, number of ADC steps and the timer interval to check the SOC.

##### Test results:

From Fig. 12, the LCD screen displays that the system is currently in the charging mode and the battery SOC is 65%. The Green LED is lit which also indicates charging mode. For verifying the discharging mode, two loads were used: the AC fan and a resistive load. When the load is the fan, it is observed that the fan takes power from the battery to run (i.e., rotate). In addition, using the resistive load, it is confirmed that the inverter’s output waveform is 120VAC and 60Hz.

While the system was charging, the current going through the LiFePo4 battery was 3.2A. Therefore, the input power would be  $P = VI = 12V \times 3.2A = 38.4W$ . When using the fan as load, the current going through the inverter is measured to be 2.95A, meaning the power output is  $P = VI = 12V \times 2.95A = 35.4W$ . This confirms proper operation of the inverter (discharging mode) because the power rating of the fan is 35W. The efficiency of the battery is determined by the ratio between the output power and input power. Hence, the battery efficiency is  $35.4/38.4 = 0.9219$  or 92.19%. This is an ideal efficiency for LiFePo4 batteries.

Overall, testing results have shown that the physical prototype works properly. It can be used in any lab for hands-on training. Furthermore, it can be used as a public demonstration tool showing how the bi-directional charging system works. The LED and the LCD display serve as effective tools to show different system operating conditions.

## 5. Conclusion

In this project, a bi-directional charger for electric vehicles has been designed, simulated, built, and tested. The results have led to the following conclusion:

- 1) A bi-directional charger is not only possible to make but also can be readily used in the near future.
- 2) The Simulink model shows that Grid-to-Vehicle and Vehicle-to-Grid modes work as desired to charge and discharge the EV battery appropriately. The physical model confirms, on a small scale, the practicality of G2V and V2G concepts.
- 3) The study contributes a new approach to EV-related training activities where both the software and physical models are developed for explaining advanced technical concepts. Additionally, the physical system is a vibrant visual tool for public education. The Simulink models have been used to teach a graduate course successfully. The physical system will be used for teaching relevant courses and the results will be reported when available.

Overall, the simulation and the physical bi-directional chargers can be effective tools for experiential teaching and for educating the general public of the EV concepts. For example, hands-on experiments can be developed using the prototype to teach students multiple concepts, such as AC-DC and DC-AC power conversion, microcontroller operation, and battery state of charge estimation. Further, demos using the prototype can help the general public understand the EV charging concepts. The overall benefit of the designed system is to help train workforce and educate the public about EVs in an easy to understand manner. This, in turn, promotes the usage of EV in both charging and discharging modes which benefit the grid and the EV owners. Wide adoption of EVs, in turn, reduces carbon emissions to make our environment clean and healthy.

### Acknowledgment

The student authors would like to thank Dr. Ha Thu Le for guiding and helping the team throughout the entire project. The team also wishes to thank the following people: Ronaldo Serrano for guiding the team through the hardware implementation process for the senior project, and Chris Chu for providing his own circuit as a reference for the simulation portion.

### References

- [1] A. Balal and M. Giesselmann, "PV to Vehicle, PV to Grid, Vehicle to Grid, and Grid to Vehicle Micro Grid System Using Level Three Charging Station," in *2022 IEEE Green Technologies Conference (GreenTech)*, 30 March-1 April 2022 2022, pp. 25-30, doi: 10.1109/GreenTech52845.2022.9772041.
- [2] "IEEE Standard for Technical Specifications of a DC Quick and Bidirectional Charger for Use with Electric Vehicles - Redline," *IEEE Std 2030.1.1-2021 (Revision of IEEE Std 2030.1.1-2015) - Redline*, pp. 1-263, 2022.
- [3] J. Donadee, R. Shaw, O. Garnett, E. Cutter, and L. Min, "Potential Benefits of Vehicle-to-Grid Technology in California: High Value for Capabilities Beyond One-Way Managed Charging," *IEEE Electrification Magazine*, vol. 7, no. 2, pp. 40-45, 2019, doi: 10.1109/MELE.2019.2908793.
- [4] R. Evode, "Modeling of Electric Grid Behaviors having Electric Vehicle charging stations with G2V and V2G Possibilities," in *2021 International Conference on Electrical, Computer, Communications and Mechatronics Engineering (ICECCME)*, 7-8 Oct. 2021 2021, pp. 1-5, doi: 10.1109/ICECCME52200.2021.9591059.
- [5] C. Liu, K. T. Chau, D. Wu, and S. Gao, "Opportunities and Challenges of Vehicle-to-Home, Vehicle-to-Vehicle, and Vehicle-to-Grid Technologies," *Proceedings of the IEEE*, vol. 101, no. 11, pp. 2409-2427, 2013, doi: 10.1109/JPROC.2013.2271951.
- [6] M. Oliinyk, J. Džmura, and D. Pál, "The impact of a electric vehicle charging on the distribution system," in *2020 21st International Scientific Conference on Electric Power Engineering (EPE)*, 19-21 Oct. 2020 2020, pp. 1-5, doi: 10.1109/EPE51172.2020.9269213.
- [7] H. B. Sassi, F. Errahimi, N. Essbai, and C. Alaoui, "V2G and Wireless V2G concepts: State of the Art and Current Challenges," in *2019 International Conference on Wireless Technologies, Embedded and Intelligent Systems (WITS)*, 3-4 April 2019 2019, pp. 1-5, doi: 10.1109/WITS.2019.8723851.
- [8] P. Spichartz, T. Brüning, and C. Sourkounis, "Procedure for Avoiding and Reducing Peak Loads at Large-scale Consumers via Bidirectional Charging of Electric Vehicles to Save Electricity Costs," in *IECON 2021 – 47th Annual Conference of the IEEE Industrial Electronics Society*, 13-16 Oct. 2021 2021, pp. 1-6, doi: 10.1109/IECON48115.2021.9589701.
- [9] X. Yan, R. En, and Y. Li, "Research on Power Supply Mode for Electric Vehicle Charging Devices in Residential Community," in *2013 IEEE Vehicle Power and Propulsion Conference (VPPC)*, 15-18 Oct. 2013 2013, pp. 1-4, doi: 10.1109/VPPC.2013.6671706.
- [10] T. Yiyun, L. Can, C. Lin, and L. Lin, "Research on Vehicle-to-Grid Technology," in *2011 International Conference on Computer Distributed Control and*



- Intelligent Environmental Monitoring*, 19-20 Feb. 2011 2011, pp. 1013-1016, doi: 10.1109/CDCIEM.2011.194.
- [11] Y. Zhiyong *et al.*, "Optimization of Orderly Charge and Discharge Scheduling of Electric Vehicles and Photovoltaic in Industrial Par," in *2020 Asia Energy and Electrical Engineering Symposium (AEEES)*, 29-31 May 2020 2020, pp. 226-229, doi: 10.1109/AEEES48850.2020.9121412.
- [12] H. C. Güldorum, Ş. İ. and O. Erdiñç, "Charging Management System for Electric Vehicles considering Vehicle-to-Vehicle (V2V) Concept," in *2020 12th International Conference on Electrical and Electronics Engineering (ELECO)*, 26-28 Nov. 2020 2020, pp. 188-192.
- [13] S. G. Selvakumar, "Electric and Hybrid Vehicles – A Comprehensive Overview," in *2021 IEEE 2nd International Conference On Electrical Power and Energy Systems (ICEPES)*, 10-11 Dec. 2021 2021, pp. 1-6, doi: 10.1109/ICEPES52894.2021.9699557.
- [14] Y. Zhou and X. Li, "Vehicle to grid technology: A review," in *2015 34th Chinese Control Conference (CCC)*, 28-30 July 2015 2015, pp. 9031-9036, doi: 10.1109/ChiCC.2015.7261068.
- [15] Y. Zhou and A. Vyas, "Keeping plug-in electric vehicles connected to the grid - Patterns of vehicle use," in *2012 IEEE PES Innovative Smart Grid Technologies (ISGT)*, 16-20 Jan. 2012 2012, pp. 1-1, doi: 10.1109/ISGT.2012.6175805.
- [16] S. T. Inc., "Power Efficiency Gains by Deploying 415 VAC Power Distribution in North American Data Centers," 2011. Accessed: 23 February 2023. [Online]. Available: [https://cdn10.servertech.com/assets/documents/documents/63/original/415VAC\\_Power\\_Distribution\\_Dec14.pdf?1452798619](https://cdn10.servertech.com/assets/documents/documents/63/original/415VAC_Power_Distribution_Dec14.pdf?1452798619)
- [17] T. R. Kuphaldt, *Lessons In Electric Circuits, Volume II - AC*: Design Science License, 2006, p. 570. [Online]. Available: <https://www.allaboutcircuits.com/assets/pdf/alternating-current.pdf>. Accessed on: 22 February 2023.
- [18] P. Chauhan, "AC to DC Converters: Features, Design & Applications", <https://how2electronics.com/ac-to-dc-converters-features-design-applications/#:~:text=The%20electrical%20circuits%20that%20transform,conversion%20for%20a%20DC%20output.>, 2022, Accessed: 23 February 2023.
- [19] T. Y. A. Solovev, "DC-to-DC Converters: Functions, Common Types & Design Principles, Applications, and Challenges." <https://www.integrasources.com/blog/dc-dc-converters-functions-types-design-applications-challenges/>, 2022, Accessed: 23 February 2023.
- [20] M. E. V. Team, "A Guide to Understanding Battery Specifications." [http://web.mit.edu/evt/summary\\_battery\\_specifications.pdf](http://web.mit.edu/evt/summary_battery_specifications.pdf), 2008, Accessed: 23 February 2023.
- [21] A. Dhage, "Rivian R1T Battery Pack Benchmarking." <https://www.batterydesign.net/rivian-r1t/#:~:text=voltage%20range%20%5BV%5D%3A,Minimum%3A%2016%20V>, 2023, Accessed: 23 February 2023.
- [22] Chris Chu and Ha Thu Le (Advisor), "Supporting Bidirectional Operation of Electric Vehicle-to-Grid, Vehicle-to-Home, and Vehicle-to-Load (Thesis)," MSEE, California State Polytechnic University Pomona, 2023.
- [23] "LiFePO4 Battery Discharge and Charge Curve." BravaBattery. <https://www.bravabatteries.com/lifepo4-battery-discharge-and-charge-curve/>, Accessed: 22 February 2023.

**APPENDIX**

Table A1. Physical System Components and Costs

<b>Description</b>	<b>Quantity</b>	<b>Cost, US\$</b>
NERMAK 12V 20Ah Lithium LiFePO4 Deep Cycle Battery	1	79.99
ULTRAPOWER 4Amp 12.8V-14.6V Lithium LifePO4 Battery Charger,4-Stage Automatic Repair Intelligent Lithium Battery Charger for Cars,Motorcycles,Lawn Mowers,Toy Cars,Golf Carts,LifePO4 Batteries	1	27.99
14 Gauge 4 Color Pack in 100 ft Roll (400 Feet Total)	1	29.15
WGGE WG-015 Professional 8-inch Wire Stripper / wire crimping tool, Wire Cutter, Wire Crimper, Cable Stripper, Wiring Tools and Multi-Function Hand Tool	1	8.59
5 Pack LM2596 DC to DC Buck Converter 3.0-40V to 1.5-35V Power Supply Step Down Module	1	8.99
NOYITO 12V 24V Battery Charging Control Board (12-24V MAX30V) Battery Charge Control Switch Auto Power Off Safe and Energy Saving	1	8.99
AEDIKO 4pcs Relay Module DC 12V Relay Board 1 Channel with Optocoupler Isolation Support High or Low Level	2	13.98
180 WATT PURE SINE INVERTER	1	86.00
NOCO GENIUS1, 1A Smart Car Battery Charger, 6V and 12V Automotive Charger, Battery Maintainer, Trickle Charger, Float Charger and Desulfator for AGM, Motorcycle, Lithium and Deep Cycle Batteries	1	29.95
2PCS 14 AWG Alligator Clips Test Leads Dual Ended Crocodile Heavy Duty Wire Cable with Insulators Clips Test Flexible Copper Cable for Electrical Testing 6.6ft	1	13.99
True RMS Digital Multimeter Tester 6000 Counts AC DC 20A Ohmmeter Voltmeter DMM Measure Voltage Current Amp Resistance Diodes Continuity Duty-Cycle Capacitance Temperature (BTMETER BT-770T)	1	29.99
WAGO 221-415 Lever-Nuts 5 Conductor Compact Connectors 10 PK	3	28.29
260PCS Heat Shrink Ring Terminals, Sopoby Marine Grade Ring Connectors Tinned Red Copper 16-14 22-18 12-10 Gauge(3 Colors/4 Sizes), 10,1/4",5/16",3/8" Insulated Ring Crimp Terminals	1	19.99
ANMBEST 5PCS 2 Channel 5V Relay Module with Optocoupler High or Low Level Trigger Expansion Board for Raspberry Pi Arduino Brand: ANMBEST	1	14.99
SEEKONE Heat Gun 1800W 122°F~1202°F (50°C- 650°C) Fast Heating Heavy Duty Hot Air Gun Kit Variable Temperature Control Overload Protection with 4 Nozzles for Crafts, Shrinking PVC, Stripping Paint(5.2FT)	1	28.99
14 AWG 3 Conductor 3-Prong Power Cord with Open Wiring, 15 Amp Max, 6 ft Replacement Power Cord with Open End, Pigtail Open Cable	1	12.99
DC Power Supply Variable 30V 6A, TOAUTO Adjustable Switching Regulated Power Supply with 4-Digit Large Display, Short Circuit Alarm, Coarse and Fine Adjustments for Lab Equipment, DIY Tool, Repair	1	59.25
KAIWEETS HT206D Digital Clamp Meter T-RMS 6000 Counts, Multimeter Voltage Tester Auto-ranging, Measures Current Voltage Temperature Capacitance Resistance Diodes Continuity Duty-Cycle (AC/DC Current)	1	51.95
Honeywell Turboforce Fan, Ht-900, 11 inch	1	18.56
Wirewound Resistors - Chassis Mount 1 KOHms 200W 30PPM	2	82.72
Wirewound Resistors - Chassis Mount 500 OHMS 1%	2	68.58
<b>TOTAL (Including Taxes and Shipping)</b>		<b>805.88</b>

**Microcontroller Arduino Code**

```
#include <LiquidCrystal.h> // includes the
LiquidCrystal Library
LiquidCrystal lcd(1, 2, 4, 5, 6, 7); // Creates an LCD
object. Parameters: (rs, enable, d4, d5, d6, d7)
```

```
double SOC = 0.05;
int SOC_Value = 0;
int bat_percent = 0;
String Status = "Idle";
int SWITCH_VALUE = 0;
int SWITCH_VALUE2 = 0;
```

```
const int PIN_RED = 11;
const int PIN_GREEN = 10;
const int PIN_BLUE = 9;
const int RELAY_1 = 8;
const int RELAY_2 = 12;
const int SWITCH = 3;
const int SWITCH2 = 13;
const int ADC_READ = A0;
int Variable = 0;
int Charging = 0;
int Discharging = 0;
void Charge();
void Discharge();
void Beginning();
void setup()
{
  pinMode(PIN_RED, OUTPUT);
  pinMode(PIN_GREEN, OUTPUT);
  pinMode(PIN_BLUE, OUTPUT);
  pinMode(ADC_READ, INPUT);
  pinMode(SWITCH, INPUT);
  pinMode(SWITCH2, INPUT);
  pinMode(RELAY_1, OUTPUT);
  pinMode(RELAY_2, OUTPUT);
  digitalWrite(RELAY_1, LOW);
  digitalWrite(RELAY_2, LOW);
```

```
lcd.begin(16,2); // Initializes the interface to the LCD
screen, and specifies the dimensions (width and
height) of the display }
}
```

```
void loop()
{
  Beginning();
```

```
if (SWITCH_VALUE == LOW)
{
  Status = "Idle";
```

```
digitalWrite(RELAY_1, LOW);
digitalWrite(RELAY_2, LOW);
digitalWrite(PIN_RED, LOW);
digitalWrite(PIN_GREEN, LOW);
digitalWrite(PIN_BLUE, HIGH);
delay(1000);
}
```

```
else if (SWITCH_VALUE2 == HIGH)
{
  Charge();
}
else if (bat_percent <= 30)
{
  Charge();
}
else if (bat_percent >= 80)
{
  Discharge();
}
else if ((bat_percent < 80 || Charging == 1) &&
Discharging == 0)
{
  Charge();
}
delay(500);
lcd.clear();
}
void Charge ()
{
  Charging = 1;
  Discharging = 0;
  Status = "Charging";
  digitalWrite(RELAY_1, HIGH);
  digitalWrite(RELAY_2, LOW);
  digitalWrite(PIN_RED, LOW);
  digitalWrite(PIN_GREEN, HIGH);
  digitalWrite(PIN_BLUE, LOW);
  lcd.setCursor(0,0);
  lcd.print(Status);
  for (int i = 0; i < 2*60; i++) //Charge for 1 minute(s)
  {
    delay(1000);
    lcd.setCursor(12,1);
    lcd.print(i+1);
  }
  digitalWrite(RELAY_1, LOW);
  digitalWrite(RELAY_2, LOW);
  delay(3000); //Wait 3 second to read battery
voltage
  Beginning();
```

```

}

void Discharge ()
{
  Charging = 0;
  Discharging = 1;
  Status = "Discharging";
  digitalWrite(RELAY_1, LOW);
  digitalWrite(RELAY_2, HIGH);
  digitalWrite(PIN_RED, HIGH);
  digitalWrite(PIN_GREEN, LOW);
  digitalWrite(PIN_BLUE, LOW);
  delay(1000);
}

void Beginning ()
{
  SOC_Value = analogRead(ADC_READ);
  if (Discharge ==1)
  {
    SOC_Value += 10;
  }

  SWITCH_VALUE = digitalRead(SWITCH);
  SWITCH_VALUE2 = digitalRead(SWITCH2);

  lcd.setCursor(12,0);
  lcd.print(SOC_Value);
  lcd.setCursor(0,0);
  lcd.print(Status);

  if (SOC_Value >= 890) bat_percent = 100;

  else if (SOC_Value >= 840) // 95-100% range
    bat_percent = map(SOC_Value, 840, 890, 95, 100);
  else if (SOC_Value >= 700) // 20-95% range
    bat_percent = map(SOC_Value, 700, 840, 20, 95);
  else if (SOC_Value >= 683) // 0-20% range
    bat_percent = map(SOC_Value, 683, 700, 0, 20);
  else bat_percent = 0;

  lcd.setCursor(0,1);
  lcd.print("SOC: ");
  lcd.print(bat_percent);
  lcd.print(" %");
}

```